



Originally published as:

Jochum, K. P., Schuessler, J. A., Wang, X.-H., Stoll, B., Weis, U., Müller, W. E. G., Haug, G. H., Andrae, M. O., Froelich, P. N. (2017): Whole-Ocean Changes in Silica and Ge/Si Ratios During the Last Deglacial Deduced From Long-Lived Giant Glass Sponges. - *Geophysical Research Letters*, 44, 22, pp. 11555—11564.

DOI: <http://doi.org/10.1002/2017GL073897>



RESEARCH LETTER

10.1002/2017GL073897

Key Points:

- Si isotope and Ge measurements in the deep-sea sponge *Monorhaphis chuni* provide an archive of climate change, reaching back to at least 17 ka B.P.
- Our data suggest that at the onset of the last deglaciation, deep Pacific Ocean dissolved silica was higher and Ge/Si lower than at present

Supporting Information:

- Supporting Information S1

Correspondence to:

K. P. Jochum,
kjochum@mpic.de

Citation:

Jochum, K. P., Schuessler, J. A., Wang, X.-H., Stoll, B., Weis, U., Müller, W. E. G., ... Froelich, P. N. (2017). Whole-ocean changes in silica and Ge/Si ratios during the last deglacial deduced from long-lived giant glass sponges. *Geophysical Research Letters*, 44, 11,555–11,564. <https://doi.org/10.1002/2017GL073897>

Received 26 APR 2017

Accepted 31 OCT 2017

Accepted article online 6 NOV 2017

Published online 23 NOV 2017

Whole-Ocean Changes in Silica and Ge/Si Ratios During the Last Deglacial Deduced From Long-Lived Giant Glass Sponges

K. P. Jochum^{1,2} , J. A. Schuessler³ , X.-H. Wang⁴, B. Stoll^{1,2}, U. Weis^{1,2} , W. E. G. Müller⁴, G. H. Haug², M. O. Andreae^{1,5} , and P. N. Froelich⁶

¹Biogeochemistry Department, MPIC Max Planck Institute for Chemistry, Mainz, Germany, ²Climate Geochemistry Department, MPIC Max Planck Institute for Chemistry, Mainz, Germany, ³GFZ German Research Centre for Geosciences, Potsdam, Germany, ⁴ERC Advanced Grant Research Group at the Institute for Physiological Chemistry, University Medical Center of the Johannes Gutenberg University Mainz, Mainz, Germany, ⁵Scripps Institution of Oceanography, University of California, San Diego, La Jolla, CA, USA, ⁶Nicholas School of the Environment, Duke University, Durham, NC, USA

Abstract Silicon is a keystone nutrient in the ocean for understanding climate change because of the importance of Southern Ocean diatoms in taking up CO₂ from the surface ocean-atmosphere system and sequestering carbon into the deep sea. Here we report on silicon isotopes and germanium-to-silicon ratios in giant glass spicules of deep-sea sponge *Monorhaphis chuni* over the past 17,000 years. In situ measurements of Si isotopes and Ge concentrations show systematic variations from rim to center of the cross sections. When calibrated against seawater concentrations using data from modern spicule rims, sponge data indicate that dissolved silica concentrations in the deep Pacific were ~12% higher during the early deglacial. These deep Pacific Ocean data help to fill an important global gap in paleo-nutrient records. Either continental sources supplied more silica to the deglacial ocean and/or biogenic silica burial was lower, both of which may have affected atmospheric CO₂.

1. Introduction

Silicon (Si) is one of three biolimiting macronutrients for marine phytoplankton growth in the ocean (with nitrogen and phosphorus), especially for siliceous diatoms that control almost 50% of the global sinking flux of carbon from the surface ocean to the deep sea. Information about variations in the silica content of the oceans over geological time is important for understanding changes in the carbon cycle and in atmospheric CO₂ and climate. However, the history of Si concentrations in the deep sea is poorly known. Silicon and its geochemical twin germanium (Ge) are depleted in the surface ocean due to diatom uptake and enriched at depth due to dissolution of sinking diatoms (Froelich & Andreae, 1981; Treguer et al., 1995). Major inputs of Si and Ge to the upper oceans derive from rivers (erosion and chemical weathering of the continental crust) and from eolian transport (Treguer et al., 1995; Treguer & De La Rocha, 2013). The deep ocean receives inputs from hydrothermal vents and low-temperature sea floor weathering (King et al., 2000). Removal from the ocean occurs primarily through the burial of diatom opal that survives dissolution on the seafloor and through reverse weathering in marine sediments (Aller, 2014; Baronas et al., 2017; Rahman et al., 2017; Treguer & De La Rocha, 2013).

Biogenic silica is an important archive recording paleo-Si and paleo-Ge in seawater (Ellwood et al., 2006; Shemesh et al., 1989). There are numerous measurements from fossil diatoms that reveal secular variations in the surface ocean (De La Rocha et al., 1998; Mortlock et al., 1991). However, changes in the deep sea have not been comprehensively studied. There are a few published data of both Ge and Si from siliceous sponges living in the deep sea (Ellwood et al., 2006, 2010; Hendry et al., 2010; Hendry & Brzezinski, 2014), but no microanalyses of both Si isotopes and Ge concentrations in living individuals or fossils from the same *single* sponge species. Such deep ocean silica proxies may help constrain present-day and past marine Si and Ge cycles and fluxes from continental crustal materials, fluxes associated with sediment diagenesis, and the role of diatoms in affecting CO₂ and climate. Here we report a novel deep ocean paleo-silica archive based on giant spicules of a long-lived *Hexactinellid* sponge. These sponges extend back in time to at least the early deglacial and are the only solitary spicule specimens that have so far been both calibrated in situ and analyzed along growth axes for paleo-proxies of silica.

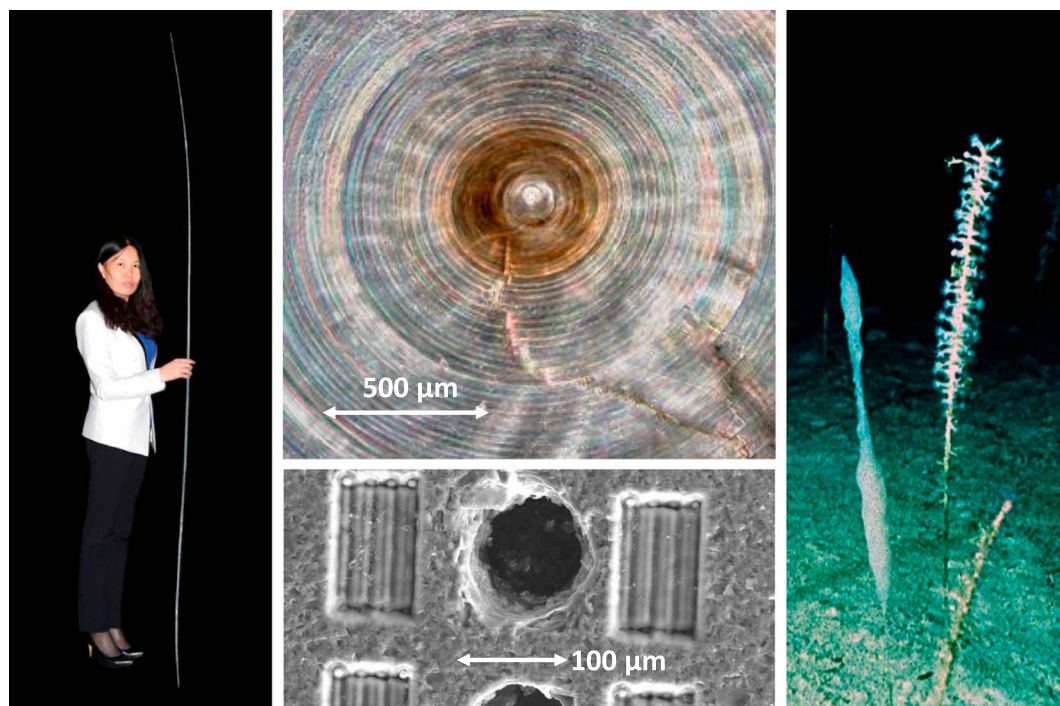


Figure 1. Giant spicule from deep-sea sponge *Monorhaphis chuni*. (left) Spicule SCS4 from the South China Sea is 2.7 m long (Wang et al., 2009). (middle) Polished cross section of SCS3-MC with femtosecond (rectangular scans) and nanosecond (round spots) laser ablation craters. (right) One meter long specimens of *M. chuni* from the South Pacific near New Caledonia living in their natural soft bottom habitat at a depth of about 1,000 m (photograph by M. Roux, University of Reims, 1991; reproduced with permission).

2. Materials and Methods

2.1. Samples and Sample Preparation

Samples were prepared from 10 segments of five giant spicules of living *Monorhaphis chuni* dredged at depths between 1,110 and 2,100 m from the East China Sea (ECS), South China Sea (SCS), and Southwest Pacific (SWPac) near New Caledonia (Table S5 and Figure S1 in the supporting information). The SCS is a semienclosed marginal sea with a short deep-water exchange time that reflects the current composition of intermediate to deep Western Pacific seawater (Chou et al., 2007). The sponges were collected from depths shallower than the controlling sill depth of the Luzon Straits (~2,200 m) with the West Equatorial Pacific. The spicules reach lengths up to 2.7 m (Figure 1) and are the largest biosilica structure on Earth (Wang et al., 2009; Wang et al., 2011).

2.2. High-Resolution Measurements

Here we report the first microanalyses of Si isotopes and Ge abundances in axial cross sections of the spicules. Each center-to-rim transect was of several millimeter length comprising multiple ~100 μm spots. Silicon isotopes were determined by UV femtosecond laser ablation coupled to a MC-ICP-MS (Neptune, Thermo Scientific) at the GFZ Potsdam. The Si isotope data are reported as $\delta^{29,30}\text{Si}$ values in per mil relative to quartz Si isotope reference material NBS 28, defined by $\delta^{29,30}\text{Si} = [(^{29,30}\text{Si}/^{28}\text{Si})_{\text{sample}} / (^{29,30}\text{Si}/^{28}\text{Si})_{\text{NBS28}} - 1] \times 1,000$. Details of the method have been previously described (Schuessler & von Blanckenburg, 2014; supporting information). Germanium concentrations were determined by LA-ICP-MS at MPIC Mainz (Jochum et al., 2011, 2012) adjacent to the Si isotope analysis using crater sizes of 110 μm (Figure 1 and supporting information).

2.3. Seawater Concentrations

We converted Si isotope data of the *M. chuni* spicules to seawater Si concentrations using our new modern calibration plot of $\delta^{30}\text{Si}$ -sponge versus dissolved $\text{Si}(\text{OH})_4$ for *M. chuni* derived from the modern (outer rim) $\delta^{30}\text{Si}$ data 1 for our samples in contact with seawater silica (Fontorbe et al., 2016; supporting information).

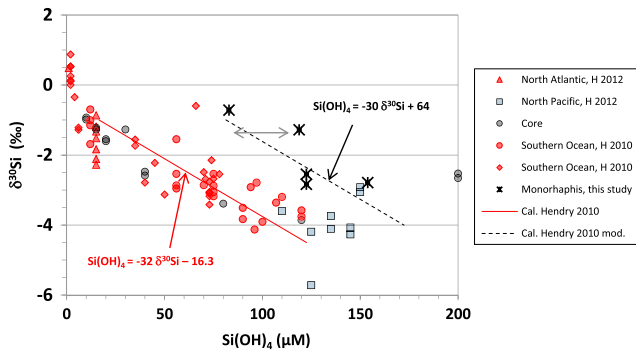


Figure 2. Sponge calibrations. Silicon isotopes of modern sponge spicules ($\delta^{30}\text{Si}$) versus dissolved silica concentrations. The red points are calibration data of handpicked (microscopic) mixed species from Wille et al. (2010), Hendry et al. (2010), and Hendry and Robinson (2012). The lightly shaded points represent “high silica” data (Griffiths et al., 2013; Hendry et al., 2014, 2012, 2015; Hendry & Robinson, 2012). The black crosses are “living” biogenic silica (outer rim in contact with seawater) of monospecific *M. chuni* samples (this paper). The solid red and dashed black lines through the two data sets are linear regressions ($r^2 > 0.80$ for each). The double-headed horizontal arrow for *M. chuni* data represents a possible downslope redeposition for sample SCS3 from 119 μM Si at the collection site to $\sim 90 \mu\text{M}$ Si at an assumed 300 to 600 m shallower growth site. Note that slopes of the two calibration lines are parallel. The equation of the published linear calibration line (Hendry et al., 2010) is $\text{Si(OH)}_4 = -30.3 (\delta^{30}\text{Si-sponge}) - 13.79$, almost identical to the “red” calibration data shown here.

Our modern calibration line (Figure 2)

$$-30 \delta^{30}\text{Si}_{\text{sponge}}\text{‰} + 64 = \text{Si(OH)}_4 (\mu\text{M}) \quad (1)$$

was then used to calculate Si(OH)_4 from nonmodern *M. chuni* biogenic $\delta^{30}\text{Si}$.

To convert spicule Ge concentrations to seawater concentrations, we used the relationship

$$(\text{Ge/Si})_{\text{spicule}} = \alpha \cdot (\text{Ge})_{\text{seawater}} + c, \quad (2)$$

where $(\text{Ge})_{\text{seawater}}$ is seawater Ge concentration, and α (0.0031 mol^{-1}) and c (-0.02) are constants (Model I of Ellwood et al., 2006). We could have inverted the process to use the modern in situ Ge and Si seawater concentrations to calibrate the Ge-spicule rims to Ge-seawater relationship, which would have given the same result. This relationship is water depth (pressure) dependent. Therefore, the analytical spicule-Ge/Si data are very different from the predicted seawater-Ge/Si values derived from this relationship. Whereas the *measured* $\delta^{30}\text{Si}$ and Ge data of the spicule rims are negatively correlated, the corresponding *derived* Si and Ge seawater concentrations are positively correlated, yielding a modern Ge/Si ratio of $0.70 \mu\text{mol mol}^{-1}$ in the SCS, ECS, and SWPac (Figures 3 and 4). This modern Ge/Si ratio is identical to that measured in present-day seawater globally (Froelich et al., 1985, 1992; Froelich & Andreae, 1981; Sutton et al., 2010)

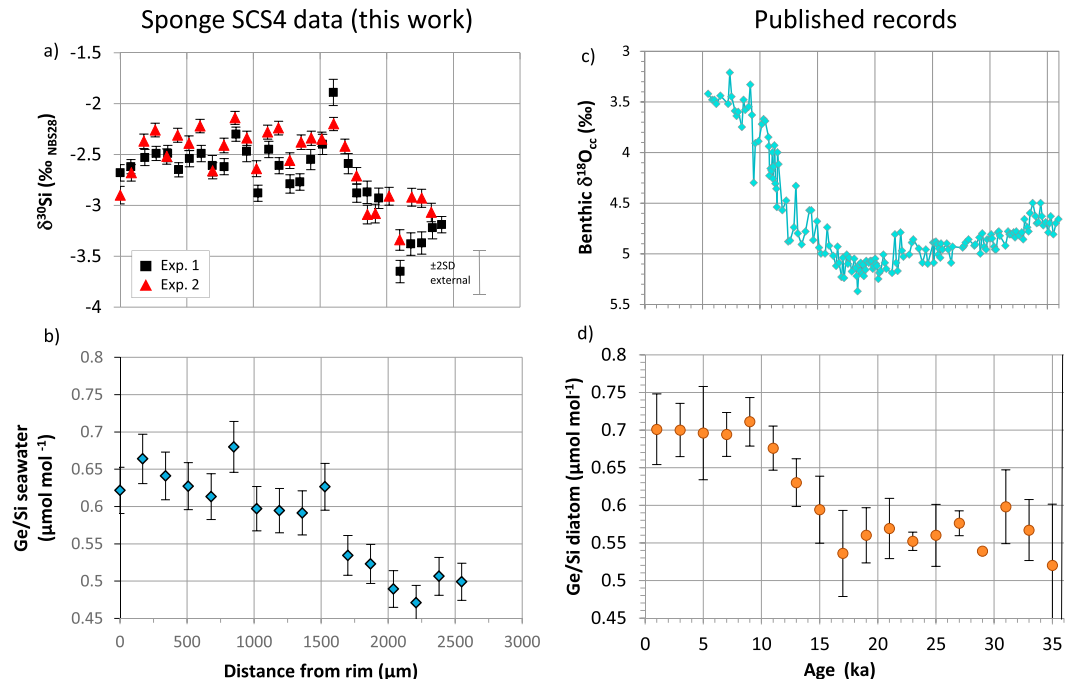


Figure 3. Comparison of SCS4 sponge data with published records. (a) $\delta^{30}\text{Si}$ in SCS4 and (b) Ge/Si in seawater deduced from $\delta^{30}\text{Si}$ and Ge in SCS4 versus rim to axis distance (increasing age). Uncertainties are explained in Figure S2. (c) The radiocarbon-dated (benthic foram-*Uvigerina* spp.) $\delta^{18}\text{O}$ record from the deep eastern equatorial Pacific core TR163-31B (Skinner & Shackleton, 2005). The glacial to interglacial shift in isotopic values is due both to decreasing ice volume (deglaial meltwater flooding the ocean) and to local warming of deep waters, shifting seawater and foram $\delta^{18}\text{O}$ values to lower interglacial values. This deglaial signal is typical of the deep ocean. (d) Contains the stacked diatom-Ge/Si record ($\pm\text{SD}$) from all published down core records (e.g., Charles et al., 1991; Ellwood & Hunter, 1999, 2000; Ferry et al., 2015; Froelich et al., 1989; Lisiecki & Raymo, 2005; Robinson et al., 2014; supporting information S1).

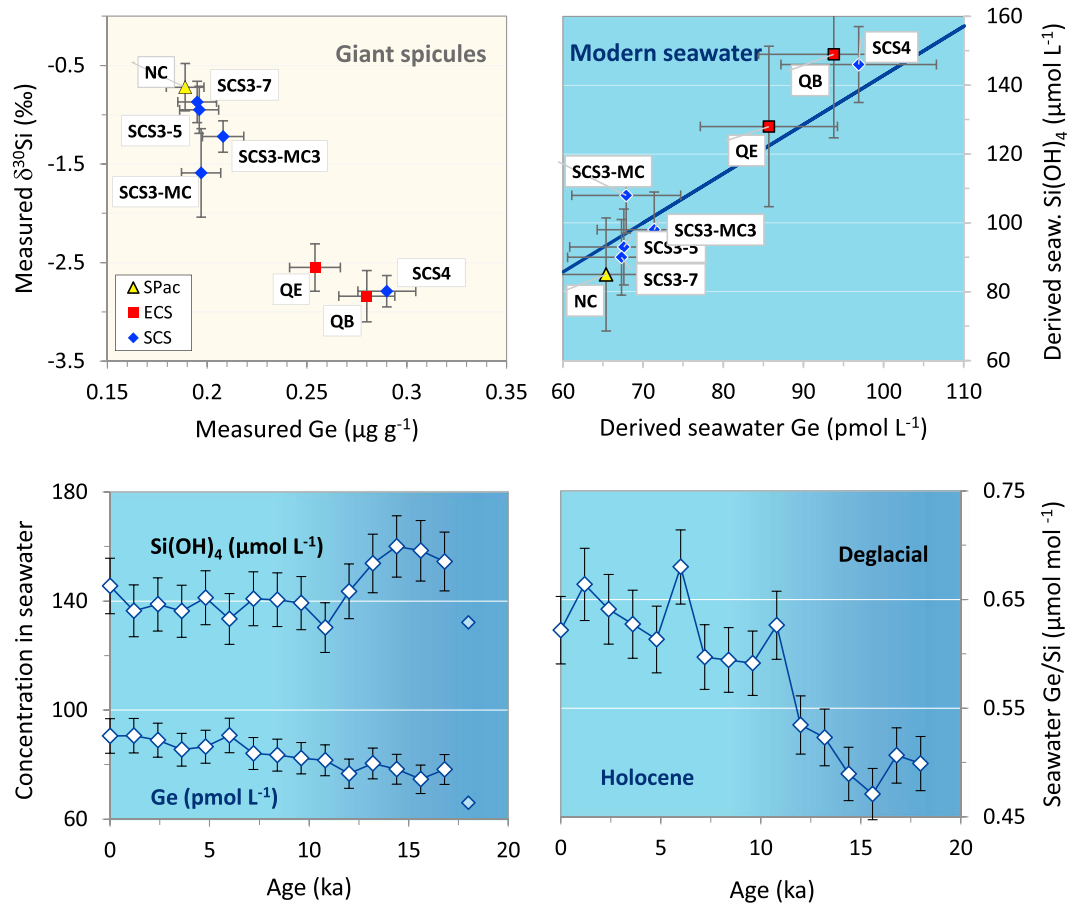


Figure 4. Silicon and germanium in giant spicules and seawater. (top left) Modern $\delta^{30}\text{Si}$ values and Ge concentrations of living spicule rims in contact with present-day seawater. (top right) These data were converted to current seawater concentrations of Si and Ge in the deep-sea. The line is the present-day Ge/Si ratio: $0.7 \mu\text{mol mol}^{-1}$ (Froelich & Andreae, 1981). (bottom left) Derived seawater Si and Ge concentrations versus age of the oldest spicule SCS4. In the deglacial period (11–18 ka B.P.) the Si concentrations are ~12% higher and Ge ~20% lower than at present. The error bars in these three figures represent overall uncertainties including statistical and calibration errors. (bottom right) Mean Ge/Si ratios ($\pm\text{SD}$) in seawater predicted from SCS4. The “oldest data” (not connected by lines) are from the central axis and may not represent the oldest silica. See supporting information for the age model.

and in modern core-top Holocene diatom shells (Figure 3) (Froelich et al., 1992; Mortlock et al., 1991; Shemesh et al., 1989).

3. Results

3.1. Si and Ge/Si Ratios in Giant Sponges

Silicon isotope ratios in biogenic silica are proxies for Si seawater concentrations because Si isotope fractionation into biogenic silica is a function of seawater Si concentration. Fractionation increases with higher Si concentration, where more negative $\delta^{30}\text{Si}$ indicates higher dissolved silica (De La Rocha, 2003; Hendry et al., 2010; Wille et al., 2010). The $\delta^{30}\text{Si}$ values for our specimens range from about -0.5‰ to -3.6‰ (Figure S2 and Tables S1b–S1i), much lower than modern ($>1,000 \text{ m}$) seawater $\delta^{30}\text{Si}$, which is about $+1.2\text{‰}$ to $+1.4\text{‰}$ in Central, Western, and South Pacific and Southern Ocean intermediate and deep waters. In addition to differences in $\delta^{30}\text{Si}$ between the specimens related to the ambient Si concentration (both ocean depth and basin), there are also systematic isotopic variations from the modern rim to the oldest center of the cross sections for all samples, especially for the largest, thickest, and oldest samples, QB and SCS4, which we interpret below as paleo-seawater Si changes. The Ge/Si ratios also vary from rim to center (Figure S2 and Tables S1b–S1i), within a range of values similar to that observed for other spicules (Ellwood et al., 2006).

3.2. Age Estimates

There is an intense debate on the life spans of siliceous sponges, in particular, for *Monorhaphis chuni* (Jochum et al., 2012; Müller et al., 2010). Direct dating methods, such as ^{32}Si (Ellwood et al., 2007) and ^{14}C (Fallon et al., 2010) are not suitable for these spicules (Adell et al., 2003; Koziol et al., 1998; Müller, 2006; Müller & Müller, 2003; Müller et al., 2004; Wang & Müller, 2006; see supporting information S1).

To obtain plausible age estimates, we compare our results for $\delta^{30}\text{Si}$ and seawater Ge/Si (Table S4) with independent paleo-markers of the glacial-interglacial termination, for example, seawater $\delta^{18}\text{O}$ (temperature and ice volume) and diatom-Ge/Si over the last 35 ka. A cross section of SCS4 shows a significant decrease of $\delta^{30}\text{Si}$ and Ge/Si at a distance of about 1,600 μm from the rim (Figures 3 and S5). This interval likely corresponds to about 11.5 ka B.P., Termination I, and the beginning of the Holocene, as suggested by the nearly identical patterns of Ge/Si in diatoms of the Atlantic and Pacific (Mortlock et al., 1991) and seawater $\delta^{18}\text{O}$. Especially promising is the parallel behavior of the Ge/Si patterns obtained from the sponge SCS4 and diatoms. We will therefore use graphical correlation of the stacked diatom-Ge/Si data as the basis to estimate the lifespan of the oldest spicules (Figure S5). This age model is pinned at three tie points: Modern, Termination I (11.5 ka), and the base of the Ge/Si-defined onset of Southern Ocean deglaciation (~ 17 ka). It assumes smooth, continuous, and uninterrupted growth rates (Figure S3) and should be considered preliminary and approximate until confirmed. Axial growth rates are about 140 $\mu\text{m}/\text{ka}$, much slower than the 4,300 year old deep sea black coral *Leiopathes* (< 500 $\mu\text{m}/\text{ka}$; Roark et al., 2009). If confirmed, SCS4 would be the oldest living skeletal animal and the longest-lived metazoan yet discovered (e.g., Druffel et al., 1995; National Geographic, 2008, <http://news.nationalgeographic.com/news/2008/04/080414-oldest-tree.html>; Piraino et al., 1996; RMTR Oldlist, n.d., <http://www.rmtr.org/oldlist.htm>; Vasek, 1980; Petralia et al., 2014).

The presence of fresh tissue on the spicules indicates that the five *M. chuni* were alive at collection. The life span of these sponges appears to be between about 6 and 18 ka (Table S5). These tie point ages may be reliable to only about $\pm 1,000$ years, but nevertheless provide the late glacial, the deglacial, and the stable Holocene record of the deep sea during the past ~ 18 ka.

3.3. Seawater Ge/Si Ratios

Our measurements of spicule cross sections provide continuous records with a potential temporal resolution of several hundred years, containing the entire Holocene and deglacial periods in the oldest spicules, SCS4 and QB. The Si isotopes and Ge abundances in these spicules change significantly with time, implying that either the dissolved Si concentration, the Si isotope composition, or the Ge/Si of the deep sea have changed with time (Figure 4). Assuming that the $\delta^{30}\text{Si}$ value of the ocean has not changed significantly (De La Rocha & Bickle, 2005; Opfergelt et al., 2013), the *derived* Si seawater concentrations are $\sim 12\%$ higher during the glacial-deglacial than at present. In contrast, the *derived* Ge glacial-deglacial seawater concentrations are about 20% lower. These glacial to interglacial Ge, Si, and Ge/Si changes are virtually identical to those reported from microscopic mélange (mixed species) spicule analyses from cores in the Atlantic and Pacific sectors of the Southern Ocean (Ellwood et al., 2010), the only other work to combine both silica isotopes and Ge/Si data in the same spicules. Similar to Ellwood's interpretations, our spicule data most likely reflect global changes in the seawater inventories of both Si and Ge.

4. Discussion

4.1. Deglaciation

One explanation for changing ocean Si and Ge during the deglaciation could be changes in riverine, glacial, and/or eolian deliveries of silica to the sea (De La Rocha et al., 1998; Froelich et al., 1992). Changes in marine sedimentary reverse weathering removing Ge into marine sediments during opal dissolution and diagenesis are also likely (King et al., 2000; McManus et al., 2003; Treguer & De La Rocha, 2013). These external changes infer global changes in glacial silica dynamics that overprint reported changes in local nutrient circulation, redistribution, and upwelling processes.

The $(\text{Ge/Si})_{\text{sponge}}$ ratio may be a better indicator of glacial/interglacial changes than absolute abundances of spicule Si and Ge, because Ge sponge contents are dependent on seawater depth (Ellwood et al., 2006). Our predictions show that Ge/Si ratios at different water depths in the SCS, ECS, and SWPac are relatively constant during the Holocene, averaging about $0.68 \mu\text{mol mol}^{-1}$, near the Holocene stacked diatom-Ge/Si record of

the past 11.5 ka (Figures 3 and 4). Significantly lower Ge/Si ratios of around $0.55 \mu\text{mol mol}^{-1}$ are observed in the early deglacial period >17 ka B.P. with a rapid increase at about 11–17 ka to the Holocene values.

The low derived $(\text{Ge/Si})_{\text{spicule}}$ in the deep glacial ocean is identical to published ratios from sedimentary diatomaceous silica formed in the glacial subantarctic surface ocean (Figure 3; Mortlock et al., 1991). The agreement of Ge/Si in both deep and surface oceans supports both our age model and also the idea of whole-ocean variations of Ge/Si (Bareille et al., 1998; Ellwood et al., 2010; Froelich et al., 1992), rather than surface ocean diatom Ge/Si fractionation processes (Mortlock et al., 1991). Glacial and deglacial periods may be characterized by higher continental chemical weathering rates (Frings et al., 2016), lower weathering intensity, lower $(\text{Ge/Si})_{\text{river}}$, and/or higher dissolved silica river fluxes with lower $\delta^{30}\text{Si}$ (Froelich et al., 1992; Opfergelt et al., 2013), as well as increases in eolian dust input (King et al., 2000; Kurtz et al., 2002; Mahowald et al., 1999). Pulses of detrital glacier flour and ice-rafted debris (IRD) delivered to the high-latitude North Atlantic during abrupt deglaciation meltwater events (Bond et al., 1993) may also have contributed to an enhanced rapid dissolved Si supply to the ocean that appeared “faster” than the “accepted” 10 ka residence time that silica would allow. This response may be similar to the transient deglacial subglacial-meltwater uranium pulses reported to have driven *rapid* whole ocean changes in $^{234}\text{U}/^{238}\text{U}$, much faster than the canonical 0.4 Ma residence time for U in today’s ocean (Chen et al., 2016). This silica change could result from a global increase in Si supply (e.g., dust: (King et al., 2000; Kurtz et al., 2002; Mahowald et al., 1999); rivers: (Froelich et al., 1992)) or a decrease in Si removal (e.g., biogenic silica burial: (Anderson et al., 2009)).

Using whole-ocean Si and Ge balance assumptions (Hammond et al., 2004; Mortlock et al., 1993; Murnane & Stallard, 1990; Wheat & McManus, 2005; supporting information) and our measured whole-ocean late glacial to deglacial Si increase of 12% and Ge/Si of $0.55 \mu\text{mol mol}^{-1}$, we estimate a Si flux from “glacial” rivers (and dust) of 12Tmol a^{-1} , about 25–35% higher than today (Rahman et al., 2017). In addition, the diagenetic Ge sink, which is responsible for removing almost 50% of the oceanic Ge inputs today (Figure S4), must have been even more important in the more-slowly ventilated glacial ocean with lower bottom water dissolved oxygen and enhanced sedimentary suboxic conditions (Jaccard et al., 2009; Sikes et al., 2000). If so, then the rapid increase in Ge- and Ge/Si-seawater during the deglaciation may have been enhanced by abrupt reduction of this sedimentary Ge sink from the deep ocean during rapid reventilation from the Southern Ocean (Anderson et al., 2009) and changes in the redox state of margin sediments during sea level rise (Jaccard et al., 2009).

An alternative possibility is that both the higher Si and the lower Ge/Si of the early deglacial ocean were driven by reduced diatom production and a resulting decline in global marine opal burial. This conjecture is controversial. Reduced burial, if not completely compensated by other losses, would leave the ocean with higher dissolved silica. Because diatom burial does not fractionate between Ge and Si, a decrease in burial would have allowed the diagenetic Ge sink, occurring at a constant rate, to drive the ocean to a lower Ge/Si ratio. If so, then a reduction in diatom production could increase ocean silica and influence phytoplankton production on a global basis.

The feedbacks among these various scenarios are complex and poorly understood but likely involve diatom production. The ocean must somehow reestablish a Si steady state by increasing biogenic silica production to counterbalance decreased burial or by increasing silica burial to counterbalance enhanced continental weathering (De La Rocha & Bickle, 2005). Si removal into marine authigenic clays (reverse weathering) is likely the ocean’s feedback between biogenic silica supply (biogenic production) and continental aluminum supply (weathering) to the seafloor (Aller, 2014). At any rate, since diatoms carry almost half of the export flux of carbon into the deep sea at a Si:C atom ratio of about 3, changes in the diatom sinking flux must also affect upper ocean and atmosphere CO_2 .

4.2. Global Ocean Paleo-Silica Changes

We thus propose that the silicon isotope records in *M. chuni* spicules during the early deglacial in the western deep Pacific represent changes in the dissolved silica content of the global ocean. There are two lines of evidence. First of all, the Pacific Ocean today contains over 50% of the volume and 70% of global ocean silica content. The Kuroshio Branch Extension circulating from the western Pacific through the Luzon Straits carries North Pacific Intermediate Water (NPIW: You, 2003; You et al., 2005) and North Pacific Deep Water (NPDW: Grasse et al., 2013) into the SCS above sill depth (about 2,200 m: Chao et al., 1996). The exchange time for deep waters is less than 100 years, so the basin is in continuous communication with the Pacific Ocean.

Thus dissolved silica concentrations and silicon isotope data in the SCS and ECS (Cao et al., 2012, 2015; Okubo et al., 2007) derive from the central North Pacific (Beucher et al., 2008; Holzer & Brzezinski, 2015; Reynolds et al., 2006). Both the NPDW and NPIW are at the “end” of today’s ocean conveyor and thus the oldest water in today’s ocean and in the glacial ocean (Sarnthein et al., 2013; Sikes et al., 2000) with the highest nutrients, highest TCO_2 , and lowest O_2 . Because the SCS is oligotrophic today and during glacial-deglacial periods (no upwelling), changes in paleo-silica concentrations below the surface mixed layer must have been imported from the open Pacific, and thus reflect the global deep ocean.

Second, there is increasing evidence for “globally near-synchronous pulses of diatom production...” (Hendry et al., 2016), documented by both increases in biogenic silica accumulation and in bottom water silica concentrations during the deglacial, particularly striking during abrupt North Atlantic surges and collapses of the Northern Hemisphere ice sheets. These silica events have been attributed to increases in local coastal upwelling (winds), enhanced local biogenic silica preservation (burial), and to increased local deep and intermediate water silica concentrations caused by changing paleo-water mass circulation patterns (Anderson et al., 2009; Bradtmiller et al., 2006, 2007; Calvo et al., 2011; Chase et al., 2003; Gil et al., 2009; Hendry et al., 2016; Hendry & Brzezinski, 2014; Hendry & Robinson, 2012; Kienast et al., 2006; Meckler et al., 2013; Romero et al., 2008; Sprenk et al., 2013). These changes have been most thoroughly studied in the Atlantic and Southern Oceans, where they are dated to the abrupt events radiating from the North Atlantic (Dansgaard-Oeschger events). Taken together, these events could reflect a global deglacial increase and drawdown in whole-ocean-dissolved silica overprinted by changes in local silica dynamics (Frings et al., 2016).

Ellwood et al. (2010) interpreted their sponge Si isotope and Ge/Si records from the glacial Southern Pacific and Atlantic Oceans as requiring a global Si increase of up to 15% and a global Ge decrease of about 25%, consistent with the magnitude and interpretations from our data. The inferred change in whole ocean $\delta^{30}\text{Si}$ due to this enhanced deglacial deep ocean silica change would be in the same direction as the change we observe in our sponge record—lower glacial-deglacial, higher interglacial—thus having the effect of magnifying the computed dissolved silica change if the continental weathering change were sufficiently large and fast enough to alter deep Pacific $\delta^{30}\text{Si}$ (De La Rocha & Bickle, 2005; Frings et al., 2016). Whether or not opal burial remained constant during the deglacial transient—in both the real ocean and in ocean models—is of course a critical aspect of connecting ocean silica to atmospheric CO_2 and climate change.

5. Conclusions

Giant spicules of the long-lived deep-sea sponge *Monorhaphis chuni* provide a unique archive of climate and deep ocean biogeochemical change, reaching back to at least 17 ka B.P. High-resolution Si isotope and Ge concentration measurements along spicule cross sections indicate significantly higher seawater Si and lower Ge concentrations and Ge/Si ratios during the deglacial and the end of the last ice age. An ocean with transient higher dissolved silica could have influenced diatom production, potentially contributing to lower atmospheric CO_2 and climate cooling.

Acknowledgments

We thank the Editor, the two anonymous reviewers, R. F. Anderson, M. J. Ellwood, C. De La Rocha, and P. Frings for valuable comments. All supporting data are included as five tables in a supporting information file.

References

- Adell, T., Nefkens, I., & Müller, W. E. G. (2003). Polarity factor ‘Frizzled’ in the demosponge *Suberites domuncula*: Identification, expression and localization of the receptor in the epithelium/pinacoderm¹. *FEBS Letters*, 554(3), 363–368. [https://doi.org/10.1016/S0014-5793\(03\)01190-6](https://doi.org/10.1016/S0014-5793(03)01190-6)
- Aller, R. C. (2014). Sedimentary diagenesis, depositional environments, and benthic fluxes. In K. K. Turekian (Ed.), *Treatise on Geochemistry*, (2nd ed., pp. 293–334). Oxford: Elsevier. <https://doi.org/10.1016/B978-0-08-095975-7.00611-2>
- Anderson, R. F., Ali, S., Bradtmiller, L. I., Nielsen, S. H. H., Fleisher, M. Q., Anderson, B. E., & Burckle, L. H. (2009). Wind-driven upwelling in the Southern Ocean and the deglacial rise in atmospheric CO_2 . *Science*, 323(5920), 1443–1448. <https://doi.org/10.1126/science.1167441>
- Bareille, G., Labracherie, M., Mortlock, R. A., Maier-Reimer, E., & Froelich, P. N. (1998). A test of (Ge/Si) opal as a paleorecorder of (Ge/Si) seawater. *Geology*, 26(2), 179–182. [https://doi.org/10.1130/0091-7613\(1998\)026%3C0179:ATOGSO%3E2.3.CO;2](https://doi.org/10.1130/0091-7613(1998)026%3C0179:ATOGSO%3E2.3.CO;2)
- Baronas, J. J., Hammond, D. E., McManus, J., Wheat, C. G., & Siebert, C. (2017). A global Ge isotope budget. *Geochimica et Cosmochimica Acta*, 203, 265–283. <https://doi.org/10.1016/j.gca.2017.01.008>
- Beucher, C. P., Brzezinski, M. A., & Jones, J. L. (2008). Sources and biological fractionation of silicon isotopes in the eastern equatorial Pacific. *Geochimica et Cosmochimica Acta*, 72(13), 3063–3073. <https://doi.org/10.1016/j.gca.2008.04.021>
- Bond, G., Broecker, W., Johnsen, S., McManus, J., Labeyrie, L., Jouzel, J., & Bonani, G. (1993). Correlations between climate records from North Atlantic sediments and Greenland ice. *Nature*, 365(6442), 143–147. <https://doi.org/10.1038/365143a0>
- Bradtmiller, L. I., Anderson, R. F., Fleisher, M. Q., & Burckle, L. H. (2006). Diatom productivity in the equatorial Pacific Ocean from the last glacial period to the present: A test of the silicic acid leakage hypothesis. *Paleoceanography*, 21, PA4201. <https://doi.org/10.1029/2006PA001282>
- Bradtmiller, L. I., Anderson, R. F., Fleisher, M. Q., & Burckle, L. H. (2007). Opal burial in the equatorial Atlantic Ocean over the last 30 ka: Implications for glacial-interglacial changes in the ocean silicon cycle. *Paleoceanography*, 22, PA4216. <https://doi.org/10.1029/2007PA001443>

- Calvo, E., Pelejero, C., Pena, L. D., Cacho, I., & Logan, G. A. (2011). Eastern equatorial Pacific productivity and related- CO_2 changes since the last glacial period. *Proceedings of the National Academy of Sciences of the United States of America*, 108(14), 5537–5541. <https://doi.org/10.1073/pnas.1009761108>
- Cao, Z., Frank, M., & Dai, M. (2015). Dissolved silicon isotopic compositions in the East China Sea: Water mass mixing vs. biological fractionation. *Limnology and Oceanography*, 60(5), 1619–1633. <https://doi.org/10.1002/lno.10124>
- Cao, Z., Frank, M., Dai, M., Grasse, P., & Ehlert, C. (2012). Silicon isotope constraints on sources and utilization of silicic acid in the northern South China Sea. *Geochimica et Cosmochimica Acta*, 97, 88–104. <https://doi.org/10.1016/j.gca.2012.08.039>
- Chao, S.-Y., Shaw, P.-T., & Wu, S. Y. (1996). Deep water ventilation in the South China Sea. *Deep Sea Research Part I: Oceanographic Research Papers*, 43(4), 445–466. [https://doi.org/10.1016/0967-0637\(96\)00025-8](https://doi.org/10.1016/0967-0637(96)00025-8)
- Charles, C. D., Froelich, P. N., Zibello, M. A., Mortlock, R. A., & Morley, J. J. (1991). Biogenic opal in Southern Ocean sediments over the last 450,000 years: Implications for surface water chemistry and circulation. *Paleoceanography*, 6(6), 697–728. <https://doi.org/10.1029/91PA02477>
- Chase, Z., Anderson, R. F., Fleisher, M. Q., & Kubik, P. W. (2003). Accumulation of biogenic and lithogenic material in the Pacific sector of the Southern Ocean during the past 40,000 years. *Deep Sea Research Part II: Topical Studies in Oceanography*, 50(3–4), 799–832. [https://doi.org/10.1016/S0967-0645\(02\)00595-7](https://doi.org/10.1016/S0967-0645(02)00595-7)
- Chen, T., Robinson, L. F., Beasley, M. P., Claxton, L. M., Andersen, M. B., Gregoire, L. J., ... Harpp, K. S. (2016). Ocean mixing and ice-sheet control of seawater $^{234}\text{U}/^{238}\text{U}$ during the last deglaciation. *Science*, 354(6312), 626–629. <https://doi.org/10.1126/science.aag1015>
- Chou, W.-C., Sheu, D. D., Chen, C. T. A., Wen, L.-S., Yang, Y., & Wei, C.-L. (2007). Transport of the South China Sea subsurface water outflow and its influence on carbon chemistry of Kuroshio waters off southeastern Taiwan. *Journal of Geophysical Research*, 112, C12008. <https://doi.org/10.1029/2007JC004087>
- De La Rocha, C. L. (2003). Silicon isotope fractionation by marine sponges and the reconstruction of the silicon isotope composition of ancient deep water. *Geology*, 31(5), 423–426. [https://doi.org/10.1130/0091-7613\(2003\)031%3C0423:SIFBMS%3E2.0.CO;2](https://doi.org/10.1130/0091-7613(2003)031%3C0423:SIFBMS%3E2.0.CO;2)
- De La Rocha, C. L., & Bickle, M. J. (2005). Sensitivity of silicon isotopes to whole-ocean changes in the silica cycle. *Marine Geology*, 217(3–4), 267–282. <https://doi.org/10.1016/j.margeo.2004.11.016>
- De La Rocha, C. L., Brzezinski, M. A., DeNiro, M. J., & Shemesh, A. (1998). Silicon-isotope composition of diatoms as an indicator of past oceanic change. *Nature*, 395(6703), 680–683. <https://doi.org/10.1038/27174>
- Druffel, E. R. M., Griffin, S., Witter, A., Nelson, E., Southon, J., Kashgarian, M., & Vogel, J. (1995). *Gerardia*: Bristlecone pine of the deep-sea? *Geochimica et Cosmochimica Acta*, 59(23), 5031–5036. [https://doi.org/10.1016/0016-7037\(95\)00373-8](https://doi.org/10.1016/0016-7037(95)00373-8)
- Ellwood, M. J., & Hunter, K. A. (1999). Determination of the Zn/Si ratio in diatom opal: A method for the separation, cleaning and dissolution of diatoms. *Marine Chemistry*, 66(3–4), 149–160. [https://doi.org/10.1016/S0304-4203\(99\)00037-7](https://doi.org/10.1016/S0304-4203(99)00037-7)
- Ellwood, M. J., & Hunter, K. A. (2000). Variations in the Zn/Si record over the last interglacial glacial transition. *Paleoceanography*, 15(5), 506–514. <https://doi.org/10.1029/1999PA000470>
- Ellwood, M. J., Kelly, M., & de Forges, B. R. (2007). Silica banding in the deep-sea lithistid sponge *Corallistes undulatus*: Investigating the potential influence of diet and environment on growth. *Limnology and Oceanography*, 52(5), 1865–1873. <https://doi.org/10.4319/lo.2007.52.5.1865>
- Ellwood, M. J., Kelly, M., Maher, W. A., & De Deckker, P. (2006). Germanium incorporation into sponge spicules: Development of a proxy for reconstructing inorganic germanium and silicon concentrations in seawater. *Earth and Planetary Science Letters*, 243(3–4), 749–759. <https://doi.org/10.1016/j.epsl.2006.01.016>
- Ellwood, M. J., Wille, M., & Maher, W. (2010). Glacial silicic acid concentrations in the Southern Ocean. *Science*, 330(6007), 1088–1091. <https://doi.org/10.1126/science.1194614>
- Fallon, S. J., James, K., Norman, R., Kelly, M., & Ellwood, M. J. (2010). A simple radiocarbon dating method for determining the age and growth rate of deep-sea sponges. *Nuclear Instruments and Methods in Physics Research Section B: Beam Interactions with Materials and Atoms*, 268(7–8), 1241–1243. <https://doi.org/10.1016/j.nimb.2009.10.143>
- Ferry, A. J., Crosta, X., Quilty, P. G., Fink, D., Howard, W., & Armand, L. K. (2015). First records of winter sea ice concentration in the southwest Pacific sector of the Southern Ocean. *Paleoceanography*, 30, 1525–1539. <https://doi.org/10.1002/2014PA002764>
- Fontorbe, G., Frings, P. J., De La Rocha, C. L., Hendry, K. R., & Conley, D. J. (2016). A silicon depleted North Atlantic since the Palaeogene: Evidence from sponge and radiolarian silicon isotopes. *Earth and Planetary Science Letters*, 453, 67–77. <https://doi.org/10.1016/j.epsl.2016.08.006>
- Frings, P. J., Clymans, W., Fontorbe, G., De La Rocha, C. L., & Conley, D. J. (2016). The continental Si cycle and its impact on the ocean Si isotope budget. *Chemical Geology*, 425, 12–36. <https://doi.org/10.1016/j.chemgeo.2016.01.020>
- Froelich, P. N., & Andreae, M. O. (1981). The marine geochemistry of germanium: Ekasilicon. *Science*, 213, 3.
- Froelich, P. N., Blanc, V., Mortlock, R. A., Chillrud, S. N., Dunstan, W., Udomkit, A., & Peng, T. H. (1992). River fluxes of dissolved silica to the ocean were higher during glacials: Ge/Si in diatoms, rivers, and oceans. *Paleoceanography*, 7(6), 739–767. <https://doi.org/10.1029/92PA02090>
- Froelich, P. N., Hambrick, G. A., Andreae, M. O., Mortlock, R. A., & Edmond, J. M. (1985). The geochemistry of inorganic germanium in natural waters. *Journal of Geophysical Research*, 90(C1), 1133–1141. <https://doi.org/10.1029/JC090iC01p01133>
- Froelich, P. N., Mortlock, R. A., & Shemesh, A. (1989). Inorganic germanium and silica in the Indian Ocean: Biological fractionation during (Ge/Si)_{OPAL} formation. *Global Biogeochemical Cycles*, 3(1), 79–88. <https://doi.org/10.1029/GB003i001p00079>
- Gil, I. M., Keigwin, L. D., & Abrantes, F. G. (2009). Deglacial diatom productivity and surface ocean properties over the Bermuda Rise, northeast Sargasso Sea. *Paleoceanography*, 24, PA4101. <https://doi.org/10.1029/2008PA001729>
- Grasse, P., Ehlert, C., & Frank, M. (2013). The influence of water mass mixing on the dissolved Si isotope composition in the eastern equatorial Pacific. *Earth and Planetary Science Letters*, 380, 60–71. <https://doi.org/10.1016/j.epsl.2013.07.033>
- Griffiths, J. D., Barker, S., Hendry, K. R., Thornalley, D. J. R., van de Fliert, T., Hall, I. R., & Anderson, R. F. (2013). Evidence of silicic acid leakage to the tropical Atlantic via Antarctic intermediate water during marine isotope stage 4. *Paleoceanography*, 28, 307–318. <https://doi.org/10.1002/palo.20030>
- Hammond, D. E., McManus, J., & Berelson, W. M. (2004). Oceanic germanium/silicon ratios: Evaluation of the potential overprint of temperature on weathering signals. *Paleoceanography*, 19, PA2016. <https://doi.org/10.1029/2003PA000940>
- Hendry, K. R., & Brzezinski, M. A. (2014). Using silicon isotopes to understand the role of the Southern Ocean in modern and ancient biogeochemistry and climate. *Quaternary Science Reviews*, 89, 13–26. <https://doi.org/10.1016/j.quascirev.2014.01.019>
- Hendry, K. R., Georg, R. B., Rickaby, R. E. M., Robinson, L. F., & Halliday, A. N. (2010). Deep ocean nutrients during the last glacial maximum deduced from sponge silicon isotopic compositions. *Earth and Planetary Science Letters*, 292(3–4), 290–300. <https://doi.org/10.1016/j.epsl.2010.02.005>

- Hendry, K. R., Gong, X., Knorr, G., Pike, J., & Hall, I. R. (2016). Deglacial diatom production in the tropical North Atlantic driven by enhanced silicic acid supply. *Earth and Planetary Science Letters*, 438, 122–129. <https://doi.org/10.1016/j.epsl.2016.01.016>
- Hendry, K. R., & Robinson, L. F. (2012). The relationship between silicon isotope fractionation in sponges and silicic acid concentration: Modern and core-top studies of biogenic opal. *Geochimica et Cosmochimica Acta*, 81, 1–12. <https://doi.org/10.1016/j.gca.2011.12.010>
- Hendry, K. R., Robinson, L. F., McManus, J. F., & Hays, J. D. (2014). Silicon isotopes indicate enhanced carbon export efficiency in the North Atlantic during deglaciation. *Nature Communications*, 5, 3107. <https://doi.org/10.1038/ncomms4107>
- Hendry, K. R., Robinson, L. F., Meredith, M. P., Mulitza, S., Chiessi, C. M., & Arz, H. (2012). Abrupt changes in high-latitude nutrient supply to the Atlantic during the last glacial cycle. *Geology*, 40(2), 123–126. <https://doi.org/10.1130/G32779.1>
- Hendry, K. R., Swann, G. E. A., Leng, M. J., Sloane, H. J., Goodwin, C., Berman, J., & Maldonado, M. (2015). Technical note: Silica stable isotopes and silicification in a carnivorous sponge *Asbestopluma* sp. *Biogeosciences*, 12(11), 3489–3498. <https://doi.org/10.5194/bg-12-3489-2015>
- Holzer, M., & Brzezinski, M. A. (2015). Controls on the silicon isotope distribution in the ocean: New diagnostics from a data-constrained model. *Global Biogeochemical Cycles*, 29, 267–287. <https://doi.org/10.1002/2014GB004967>
- Jaccard, S. L., Galbraith, E. D., Sigman, D. M., Haug, G. H., Francois, R., Pedersen, T. F., ... Thierstein, H. R. (2009). Subarctic Pacific evidence for a glacial deepening of the oceanic respired carbon pool. *Earth and Planetary Science Letters*, 277(1–2), 156–165. <https://doi.org/10.1016/j.epsl.2008.10.017>
- Jochum, K. P., Wang, X., Vennemann, T. W., Sinha, B., & Müller, W. E. G. (2012). Siliceous deep-sea sponge *Monorhaphis Chuni*: A potential paleoclimate archive in ancient animals. *Chemical Geology*, 300–301, 143–151.
- Jochum, K. P., Weis, U., Stoll, B., Kuzmin, D., Yang, Q., Raczek, I., ... Enzweiler, J. (2011). Determination of reference values for NIST SRM 610–617 glasses following ISO guidelines. *Geostandards and Geoanalytical Research*, 35(4), 397–429. <https://doi.org/10.1111/j.1751-908X.2011.00120.x>
- Kienast, M., Kienast, S. S., Calvert, S. E., Eglinton, T. I., Mollenhauer, G., Francois, R., & Mix, A. C. (2006). Eastern Pacific cooling and Atlantic overturning circulation during the last deglaciation. *Nature*, 443(7113), 846–849. <https://doi.org/10.1038/nature05222>
- King, S. L., Froelich, P. N., & Jahnke, R. A. (2000). Early diagenesis of germanium in sediments of the Antarctic South Atlantic: In Search of the Missing Ge Sink. *Geochimica et Cosmochimica Acta*, 64, 1375–1390.
- Kozioł, C., Borojevic, R., Steffen, R., & Müller, W. E. G. (1998). Sponges (Porifera) model systems to study the shift from immortal to senescent somatic cells: The telomerase activity in somatic cells. *Mechanisms of Ageing and Development*, 100(2), 107–120. [https://doi.org/10.1016/S0047-6374\(97\)00120-6](https://doi.org/10.1016/S0047-6374(97)00120-6)
- Kurtz, A. C., Derry, L. A., & Chadwick, O. A. (2002). Germanium-silicon fractionation in the weathering environment. *Geochimica et Cosmochimica Acta*, 66(9), 1525–1537. [https://doi.org/10.1016/S0016-7037\(01\)00869-9](https://doi.org/10.1016/S0016-7037(01)00869-9)
- Lisiecki, L. E., & Raymo, M. E. (2005). A Pliocene-Pleistocene stack of 57 globally distributed benthic $\delta^{18}\text{O}$ records. *Paleoceanography*, 20, PA1003. <https://doi.org/10.1029/2004PA001071>
- Mahowald, N., Kohfeld, K., Hansson, M., Balkanski, Y., Harrison, S. P., Prentice, I. C., ... Rodhe, H. (1999). Dust sources and deposition during the last glacial maximum and current climate: A comparison of model results with paleodata from ice cores and marine sediments. *Journal of Geophysical Research*, 104, 15,895–15,916. <https://doi.org/10.1029/1999JD900084>
- McManus, J., Hammond, D. E., Cummins, K., Klinkhammer, G. P., & Berelson, W. M. (2003). Diagenetic Ge-Si fractionation in continental margin environments: Further evidence for a nonopal Ge sink. *Geochimica et Cosmochimica Acta*, 67(23), 4545–4557. [https://doi.org/10.1016/S0016-7037\(03\)00385-5](https://doi.org/10.1016/S0016-7037(03)00385-5)
- Meckler, A. N., Sigman, D. M., Gibson, K. A., Francois, R., Martinez-Garcia, A., Jaccard, S. L., ... Haug, G. H. (2013). Deglacial pulses of deep-ocean silicate into the subtropical North Atlantic Ocean. *Nature*, 495(7442), 495–498. <https://doi.org/10.1038/nature12006>
- Mortlock, R. A., Charles, C. D., Froelich, P. N., Zibello, M. A., Saltzman, J., Hays, J. D., & Burckle, L. H. (1991). Evidence for lower productivity in the Antarctic Ocean during the last glaciation. *Nature*, 351(6323), 220–223. <https://doi.org/10.1038/351220a0>
- Mortlock, R. A., Froelich, P. N., Feely, R. A., Massoth, G. J., Butterfield, D. A., & Lupton, J. E. (1993). Silica and germanium in Pacific Ocean hydrothermal vents and plumes. *Earth and Planetary Science Letters*, 119(3), 365–378. [https://doi.org/10.1016/0012-821X\(93\)90144-X](https://doi.org/10.1016/0012-821X(93)90144-X)
- Müller, W. E. G. (2006). The stem cell concept in sponges (Porifera): Metazoan traits. *Seminars in Cell & Developmental Biology*, 17(4), 481–491. <https://doi.org/10.1016/j.semcdb.2006.05.006>
- Müller, W. E. G., & Müller, I. M. (2003). Origin of the metazoan immune system: Identification of the molecules and their functions in sponges. *Integrative and Comparative Biology*, 43(2), 281–292. <https://doi.org/10.1093/icb/43.2.281>
- Müller, W. E., Wang, X., Sinha, B., Wiens, M., Schroder, H. C., & Jochum, K. P. (2010). NanoSIMS: Insights into the organization of the proteinaceous scaffold within Hexactinellid sponge spicules. *Chembiochem: A European Journal of Chemical Biology*, 11(8), 1077–1082. <https://doi.org/10.1002/cbic.201000078>
- Müller, W. E. G., Wiens, M., Adell, T., Gamulin, V., Schröder, H. C., & Müller, I. M. (2004). Bauplan of Urmetazoa: Basis for genetic complexity of Metazoa. In *International Review of Cytology* (pp. 53–92). Academic Press.
- Murnane, R. J., & Stallard, R. F. (1990). Germanium and silicon in rivers of the Orinoco drainage basin. *Nature*, 344(6268), 749–752. <https://doi.org/10.1038/344749a0>
- National Geographic (2008). <http://news.nationalgeographic.com/news/2008/04/080414-oldest-tree.html>
- Okubo, A., Obata, H., Gamo, T., Minami, H., & Yamada, M. (2007). Scavenging of ^{230}Th in the Sulu Sea. *Deep Sea Research Part II: Topical Studies in Oceanography*, 54(1–2), 50–59. <https://doi.org/10.1016/j.dsr2.2006.02.016>
- Opfergelt, S., Burton, K. W., Pogge von Strandmann, P. A. E., Gislason, S. R., & Halliday, A. N. (2013). Riverine silicon isotope variations in glaciated basaltic terrains: Implications for the Si delivery to the ocean over glacial–interglacial intervals. *Earth and Planetary Science Letters*, 369–370, 211–219.
- Petralia, R. S., Mattson, M. P., & Yao, P. J. (2014). Aging and longevity in the simplest animals and the quest for immortality. *Ageing Research Reviews*, 16, 66–82. <https://doi.org/10.1016/j.arr.2014.05.003>
- Piraino, S., Boero, F., Aeschbach, B., & Schmid, V. (1996). Reversing the life cycle: Medusae transforming into polyps and cell transdifferentiation in *Turritopsis nutricula* (Cnidaria, Hydrozoa). *Biological Bulletin*, 190(3), 302–312. <https://doi.org/10.2307/1543022>
- Rahman, S., Aller, R. C., & Cochran (2017). The missing silica sink: Revisiting the marine sedimentary Si cycle using cosmogenic ^{32}Si . *Global Biogeochemical Cycles*, 31, 1559–1578. <https://doi.org/10.1002/2017GB005746>
- Reynolds, B. C., Frank, M., & Halliday, A. N. (2006). Silicon isotope fractionation during nutrient utilization in the North Pacific. *Earth and Planetary Science Letters*, 244(1–2), 431–443. <https://doi.org/10.1016/j.epsl.2006.02.002>
- Roark, E. B., Guilderson, T. P., Dunbar, R. B., Fallon, S. J., & Mucciarone, D. A. (2009). Extreme longevity in proteinaceous deep-sea corals. *Proceedings of the National Academy of Sciences of the United States of America*, 106(13), 5204–5208. <https://doi.org/10.1073/pnas.0810875106>

- Robinson, R. S., Brzezinski, M. A., Beucher, C. P., Horn, M. G. S., & Bedsole, P. (2014). The changing roles of iron and vertical mixing in regulating nitrogen and silicon cycling in the Southern Ocean over the last glacial cycle. *Paleoceanography*, *29*, 1179–1195. <https://doi.org/10.1002/2014PA002686>
- Romero, O. E., Kim, J.-H., & Donner, B. (2008). Submillennial-to-millennial variability of diatom production off Mauritania, NW Africa, during the last glacial cycle. *Paleoceanography*, *23*, PA3218. <https://doi.org/10.1029/2008PA001601>
- Sarnthein, M., Schneider, B., & Grootes, P. M. (2013). Peak glacial ^{14}C ventilation ages suggest major draw-down of carbon into the abyssal ocean. *Climate of the Past*, *9*(6), 2595–2614. <https://doi.org/10.5194/cp-9-2595-2013>
- Schuessler, J. A., & von Blanckenburg, F. (2014). Testing the limits of micro-scale analyses of Si stable isotopes by femtosecond laser ablation multicollector inductively coupled plasma mass spectrometry with application to rock weathering. *Spectrochimica Acta Part B: Atomic Spectroscopy*, *98*, 1–18. <https://doi.org/10.1016/j.sab.2014.05.002>
- Shemesh, A., Mortlock, R. A., & Froelich, P. N. (1989). Late Cenozoic Ge/Si record of marine biogenic opal: Implications for variations of riverine fluxes to the ocean. *Paleoceanography*, *4*(3), 221–234. <https://doi.org/10.1029/PA004i003p00221>
- Sikes, E. L., Samson, C. R., Guilderson, T. P., & Howard, W. R. (2000). Old radiocarbon ages in the southwest Pacific Ocean during the last glacial period and deglaciation. *Nature*, *405*(6786), 555–559. <https://doi.org/10.1038/35014581>
- Skinner, L. C., & Shackleton, N. J. (2005). An Atlantic lead over Pacific deep-water change across Termination I: implications for the application of the marine isotope stage stratigraphy. *Quaternary Science Reviews*, *24*, 571–580.
- Sprenk, D., Weber, M. E., Kuhn, G., Rosén, P., Frank, M., Molina-Kescher, M., ... Röhling, H.-G. (2013). Southern Ocean bioproductivity during the last glacial cycle—New detection method and decadal-scale insight from the Scotia Sea. *Geological Society, London, Special Publications*, *381*(1), 245–261. <https://doi.org/10.1144/SP381.17>
- Sutton, J., Ellwood, M. J., Maher, W. A., & Croot, P. L. (2010). Oceanic distribution of inorganic germanium relative to silicon: Germanium discrimination by diatoms. *Global Biogeochemical Cycles*, *24*, GB2017. <https://doi.org/10.1029/2009GB003689>
- Treguer, P. J., & De La Rocha, C. L. (2013). The world ocean silica cycle. *Annual Review of Marine Science*, *5*(1), 477–501. <https://doi.org/10.1146/annurev-marine-121211-172346>
- Treguer, P., Nelson, D. M., Van Bennekom, A. J., Demaster, D. J., Leynaert, A., & Queguiner, B. (1995). The silica balance in the world ocean: A reestimate. *Science*, *268*(5209), 375–379. <https://doi.org/10.1126/science.268.5209.375>
- Vasek, F. C. (1980). Creosote bush: Long-lived clones in the Mojave Desert. *American Journal of Botany*, *67*(2), 246–255. <https://doi.org/10.2307/2442649>
- Wang, X., Gan, L., Jochum, K. P., Schröder, H. C., & Müller, W. E. G. (2011). The largest bio-silica structure on Earth: The giant basal spicule from the deep-sea glass sponge *Monorhaphis chuni*. *Evidence-based Complementary and Alternative Medicine*, *2011*, 14.
- Wang, X., & Müller, W. E. G. (2006). Molecular morphogenesis: Gene expression patterns in animals. In *Reviews in Cell Biology and Molecular Medicine* (pp. 269–310). KGA: Wiley-VCH Verlag GmbH & Co.
- Wang, X., Schroder, H. C., & Müller, W. E. (2009). Giant siliceous spicules from the deep-sea glass sponge *Monorhaphis chuni*. *International Review of Cell and Molecular Biology*, *273*, 69–115. [https://doi.org/10.1016/S1937-6448\(08\)01803-0](https://doi.org/10.1016/S1937-6448(08)01803-0)
- Wheat, C. G., & McManus, J. (2005). The potential role of ridge-flank hydrothermal systems on oceanic germanium and silicon balances. *Geochimica et Cosmochimica Acta*, *69*(8), 2021–2029. <https://doi.org/10.1016/j.gca.2004.05.046>
- Wille, M., Sutton, J., Ellwood, M. J., Sambridge, M., Maher, W., Eggins, S., & Kelly, M. (2010). Silicon isotopic fractionation in marine sponges: A new model for understanding silicon isotopic variations in sponges. *Earth and Planetary Science Letters*, *292*(3–4), 281–289. <https://doi.org/10.1016/j.epsl.2010.01.036>
- You, Y. (2003). The pathway and circulation of North Pacific Intermediate Water. *Geophysical Research Letters*, *30*, 2291. <https://doi.org/10.1029/2003GL018561>
- You, Y., Chern, C.-S., Yang, Y., Liu, C.-T., Liu, K.-K., & Pai, S.-C. (2005). The South China Sea, a cul-de-sac of North Pacific Intermediate Water. *Journal of Oceanography*, *61*(3), 509–527. <https://doi.org/10.1007/s10872-005-0059-6>